

NUCLEAR STRUCTURE EFFECTS ON  $\alpha$  REDUCED WIDTHS

K. S. Toth, Y. A. Ellis-Akovali, H. J. Kim, and J. W. McConnell  
Oak Ridge National Laboratory, Oak Ridge, TN 37831 USA

H. K. Carter  
UNISOR, Oak Ridge, TN 37831 USA

CONF-870970--2

DE87 014796

D. M. Moltz  
Lawrence Berkeley Laboratory, Berkeley, CA 94720 USA

## ABSTRACT

A review of  $\alpha$  widths for s-wave transitions is presented together with a discussion of the following topics: 1) a new determination of the  $^{218}\text{Ra}$  half-life and its relation to reflection asymmetry in nuclei near  $N = 130$ , 2) a measurement of the  $^{194}\text{Pb}$   $\alpha$ -decay rate and the influence of the  $Z = 82$  gap on neutron-deficient Pb nuclei and 3) an up-date of  $\alpha$ -decay-rate systematics for isotopes in the rare earth and medium-weight mass regions.

## I. Introduction

Alpha-decay transitions between ground states of doubly-even nuclei are taken to represent unhindered decays. Reduced widths for these s-wave transitions behave in a regular fashion as a function of both neutron and atomic number. They are largest for nuclei two or four particles beyond a closed shell (with sharp minima at the shell) and they then decrease as the next closure is approached.

This is shown in Fig. 1 where s-wave widths for nuclei with  $Z$  from 78 to 100 are plotted as a function of  $N$ . In our discussion,  $\alpha$ -decay rates are considered within the theoretical framework developed by Rasmussen.<sup>1</sup> Here the reduced width,  $\delta^2$ , is defined as;  $\delta^2 = \lambda h/P$ , where  $\lambda$  is the decay constant,  $h$  is Planck's constant, and  $P$  is the penetrability factor for the  $\alpha$  particle to tunnel through a barrier. One sees the regularity of the reduced widths as a function of neutron number with the extremely sharp break at  $N = 126$ . This discontinuity has been shown to be a shell structure effect (see e.g. Ref. 2). A less pronounced minimum is seen at the subshell closure at  $N = 152$ .

## II. Alpha-decay Widths and Nuclear Asymmetry

Interwoven bands of low-lying negative and positive parity levels, connected by enhanced E1 transitions, provide evidence that light radium and thorium isotopes have reflection asymmetry. Two explanations have been posited for the asymmetry, namely, static octupole deformation or  $\alpha$  clustering on the nuclear surface. One set of supporting data for the second explanation consists of rather large  $\alpha$ -decay reduced widths for nuclei in this  $N > 130$  region.

**MASTER**

DISTRIBUTION OF THIS DOCUMENT IS UNLIMITED

The submitted manuscript has been authored by a contractor of the U.S. Government under contract No. DE-AC05-84OR21400. Accordingly, the U.S. Government retains a nonexclusive, royalty-free license to publish or reproduce the published form of this contribution, or allow others to do so, for U.S. Government purposes.

## **DISCLAIMER**

This report was prepared as an account of work sponsored by an agency of the United States Government. Neither the United States Government nor any agency thereof, nor any of their employees, makes any warranty, express or implied, or assumes any legal liability or responsibility for the accuracy, completeness, or usefulness of any information, apparatus, product, or process disclosed, or represents that its use would not infringe privately owned rights. Reference herein to any specific commercial product, process, or service by trade name, trademark, manufacturer, or otherwise does not necessarily constitute or imply its endorsement, recommendation, or favoring by the United States Government or any agency thereof. The views and opinions of authors expressed herein do not necessarily state or reflect those of the United States Government or any agency thereof.

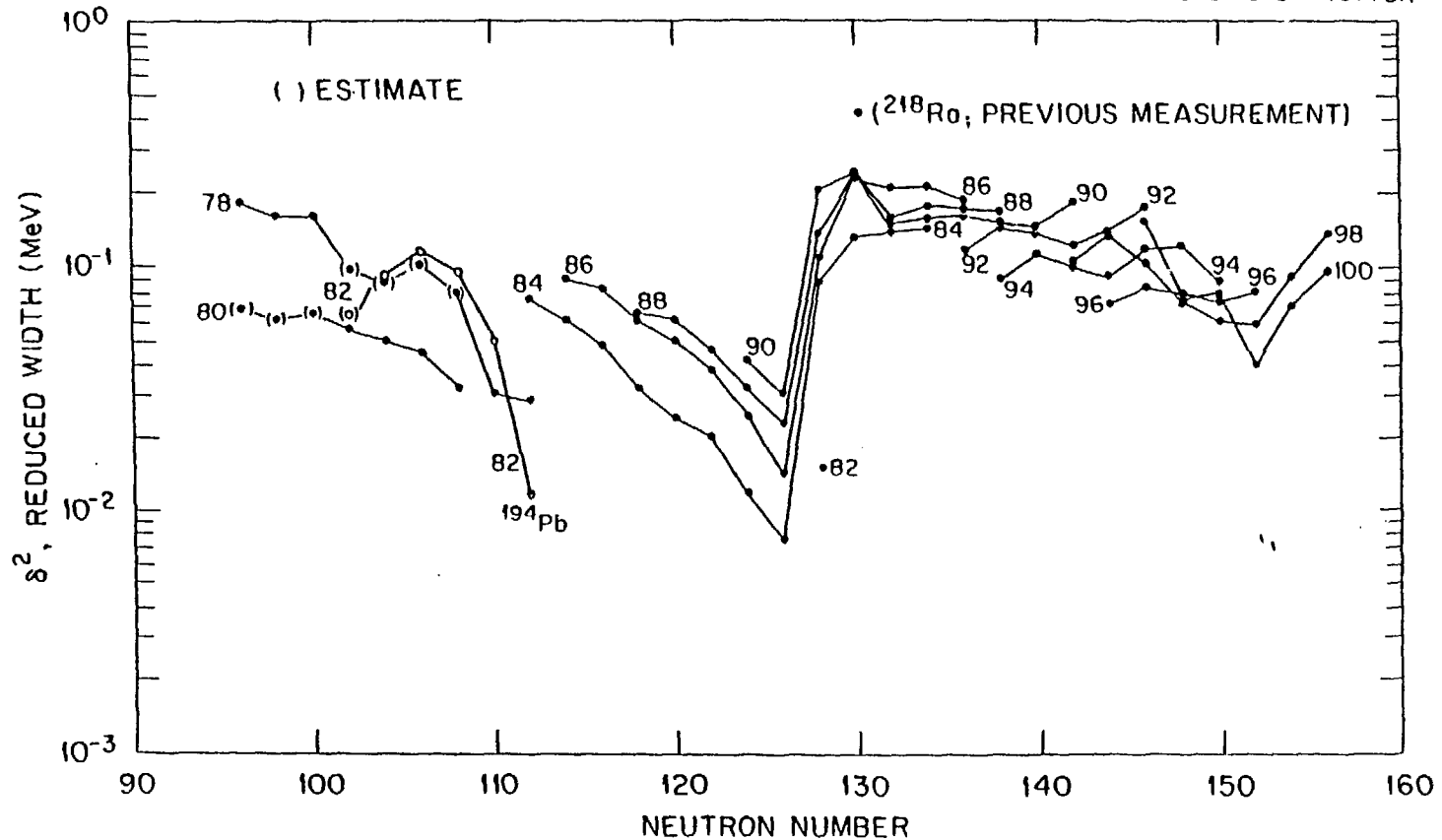


Fig. 1. Reduced widths for s-wave  $\alpha$  transitions plotted as a function of  $N$  for even-even isotopes with  $Z$  from 78 to 100. The point at  $N = 130$ , labeled as  $^{218}\text{Ra}$ , is the width calculated by using the data of Ref. 5. Widths for Pb nuclei are indicated by open points.

The  $^{218}\text{Ra}$  width, in particular, exhausts about 75% of the Wigner-sum-rule limit. This is seen in Fig. 1 where the indication is that the  $^{218}\text{Ra}$  value (open point at  $N = 130$ ) is far too large with respect to other neighboring widths. It is about a factor of two greater than the  $\delta^2$  value expected from systematics.

The  $^{218}\text{Ra}$   $\alpha$ -decay half-life was recently remeasured<sup>3</sup> at the Holifield Heavy Ion Research Facility (HHIRF) with a novel experimental technique<sup>4</sup> using a velocity filter. The  $^{218}\text{Ra}$  activity was produced by bombarding a  $^{208}\text{Pb}$  target with a  $^{13}\text{C}$  beam from the tandem accelerator. Reaction products, including the  $^{218}\text{Ra}$  nuclei, were implanted in a surface barrier detector after they had been separated from the direct accelerator beam. The implantation process provided a start signal for a calibrated time spectrum while subsequent  $\alpha$  decays supplied the stop signal.

In Fig. 2 we display some of the energy and time distributions that were obtained. Parts (a) and (b) of Fig. 2 show the spectra of heavy recoils and  $\alpha$  particles, respectively, recorded in the Si(Au) detector during the experiment. The three  $\alpha$  groups in Fig. 2(b) are  $^{218}\text{Ra}$ , its  $\alpha$ -decay daughter  $^{214}\text{Rn}$ , and a peak which encompasses events wherein both  $\alpha$  energies are summed because of the short, 0.27- $\mu\text{s}$ , half-life of  $^{214}\text{Rn}$ . As a result of the 2- $\mu\text{s}$  flight time through the velocity filter most of the short-lived  $^{214}\text{Rn}$  nuclei have to arise from  $^{218}\text{Ra}$  decay rather than from independent production. Since the  $\alpha$  branch of  $^{214}\text{Rn}$  is 100%, this is indeed reflected in the essentially equal intensities of the  $^{218}\text{Ra}$  and  $^{214}\text{Ra}$   $\alpha$  groups in Fig. 2(b).

Within uncertainties all three peaks had the same half-life, which was almost a factor of two larger than the 14- $\mu\text{s}$  value previously reported<sup>5</sup> for  $^{218}\text{Ra}$ . Figure 2(c) represents the time distribution for all  $\alpha$  decays recorded in Fig. 2(b) spread over the 80- $\mu\text{s}$  TAC range. The decay curve generated by setting gates only on the three peaks is shown in Fig. 2(d); the resultant half-life is  $25.6 \pm 1.1 \mu\text{s}$ . From this longer half-life we deduce a  $\delta^2$  value of 0.23 MeV which, in Fig. 1, is indistinguishable from the  $^{216}\text{Rn}$  and  $^{220}\text{Th}$  points. The result is a smooth trend of  $\alpha$  widths from the  $N = 130$  region to the well-deformed, prolate, Cm, Cf, and Fm nuclei, and weakens the argument for the existence of  $\alpha$  clusters in the heavy elements. (See Ref. 3 for a more complete discussion.)

To broaden the applicability of this technique to  $\alpha$  emitters with longer half-lives we devised a clock for time measurements in the ms regime. Here the  $\alpha$ -decay events are tagged with a signal from a clock that is started when the evaporation residue is implanted and reset each time that an  $\alpha$ -particle event within the expected energy range is registered. Should the  $\alpha$ -decay event not occur within a preset time range the clock is automatically reset to await a new start pulse. This clock has been tried out successfully with half-lives in the range from 1 to 100 ms. One such test involved the investigation of light thorium isotopes produced in oxygen bombardments of lead targets. Figure 3 shows the  $\alpha$ -particle spectrum observed in 90-MeV  $^{18}\text{O}$  irradiations of  $^{207}\text{Pb}$ . In that

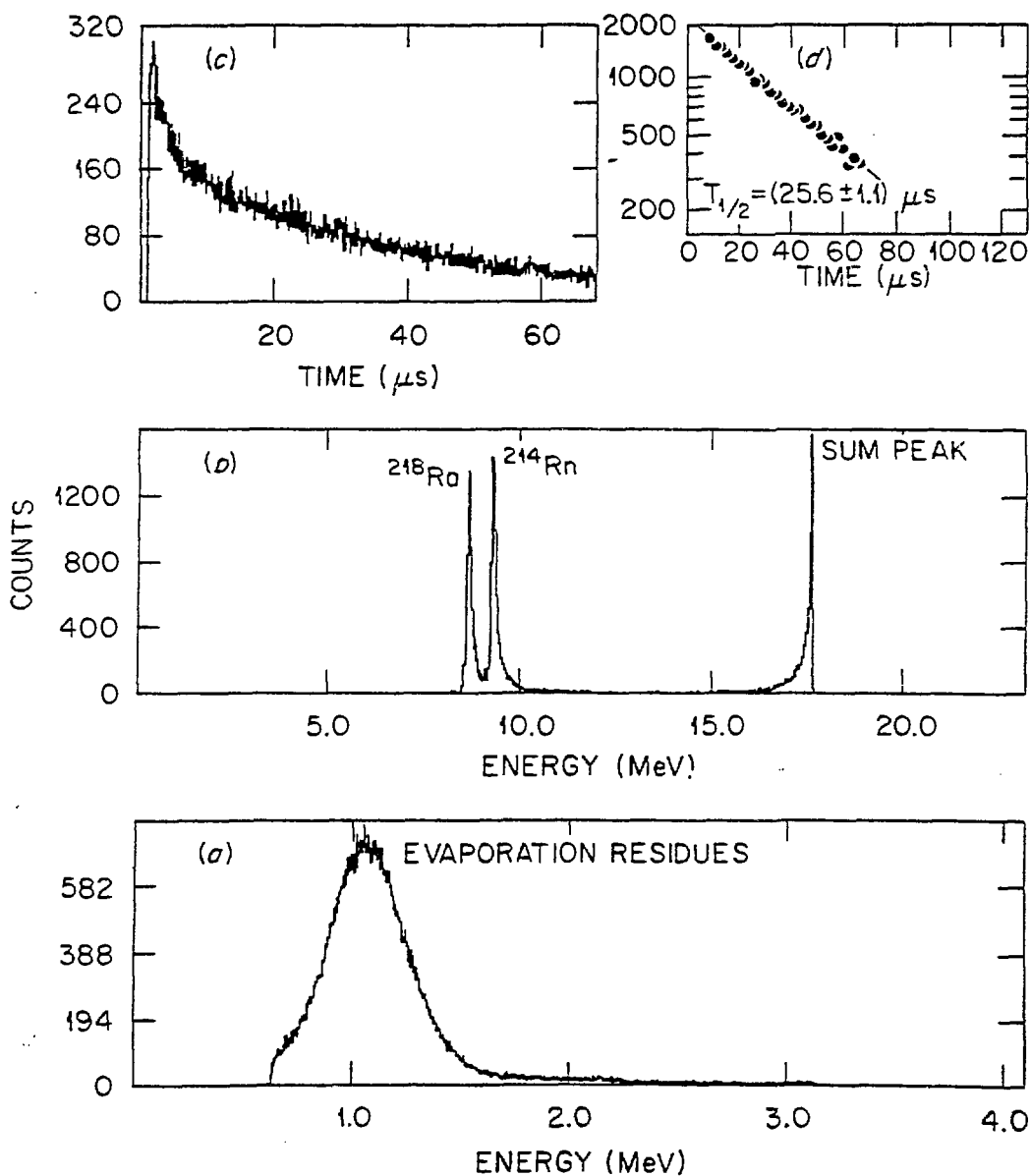


Fig. 2. Energy and time distributions measured in  $^{13}\text{C}$  bombardments of  $^{208}\text{Pb}$  after the product recoils had passed through the HHIRF velocity filter. Energy spectra recorded for products stopped in a Si(Au) surface barrier detector are shown in part (a), while subsequent  $\alpha$ -particle decays registered in the same detector are shown in part (b). Part (c) is the time distribution of all recorded  $\alpha$  decays while part (d) shows the decay curve deduced from the time distribution gated by just the three  $\alpha$  peaks in part (b).

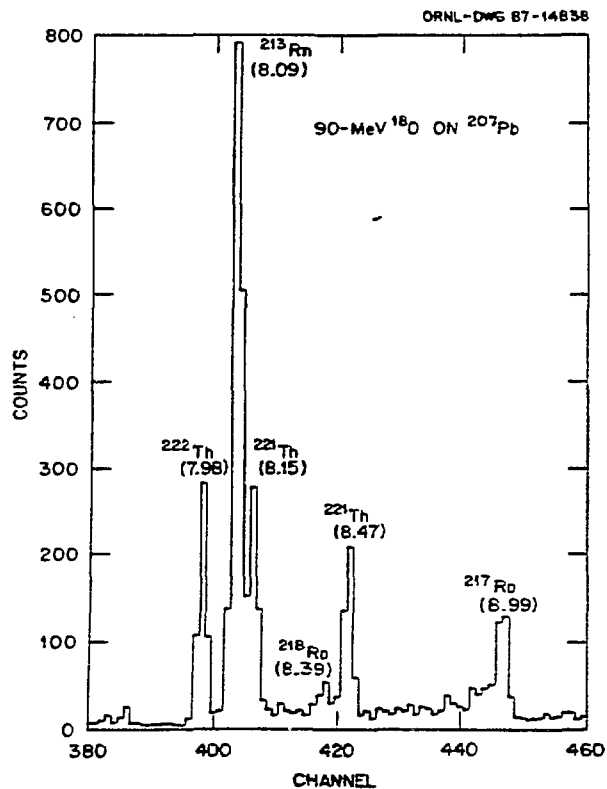


Fig. 3. Spectra recorded in a Si(Au) detector of  $\alpha$ -particles emitted by implanted residues produced in  $^{18}\text{O}$  bombardments of  $^{207}\text{Pb}$ .

study the half-lives of  $^{221}\text{Th}$  and  $^{222}\text{Th}$  were determined to be  $1.8 \pm 0.1$  and  $2.7 \pm 0.2$  ms, respectively, in agreement with published values. We plan to expand our capabilities further by using a position sensitive solid state detector so that site information can be obtained to assist in establishing parent-daughter-granddaughter decay correlations.

### III. Alpha-decay Rates of Neutron-deficient Lead Isotopes

We recently discussed<sup>6</sup> the s-wave widths of  $^{186}, ^{188}, ^{190}, ^{192}\text{Pb}$ . These widths were found to have a dependence on N similar to that observed for other neighboring elements, i.e., they decreased in value as the N = 126 shell was approached. However, contrary to the expectation of a shell effect on  $\alpha$ -decay rates at Z = 82, they were larger than those of mercury isotopes with the same neutron numbers. We suggested that this result could be related to a predicted<sup>7</sup> disappearance of the Z = 82 gap midway between N = 82 and N = 126.

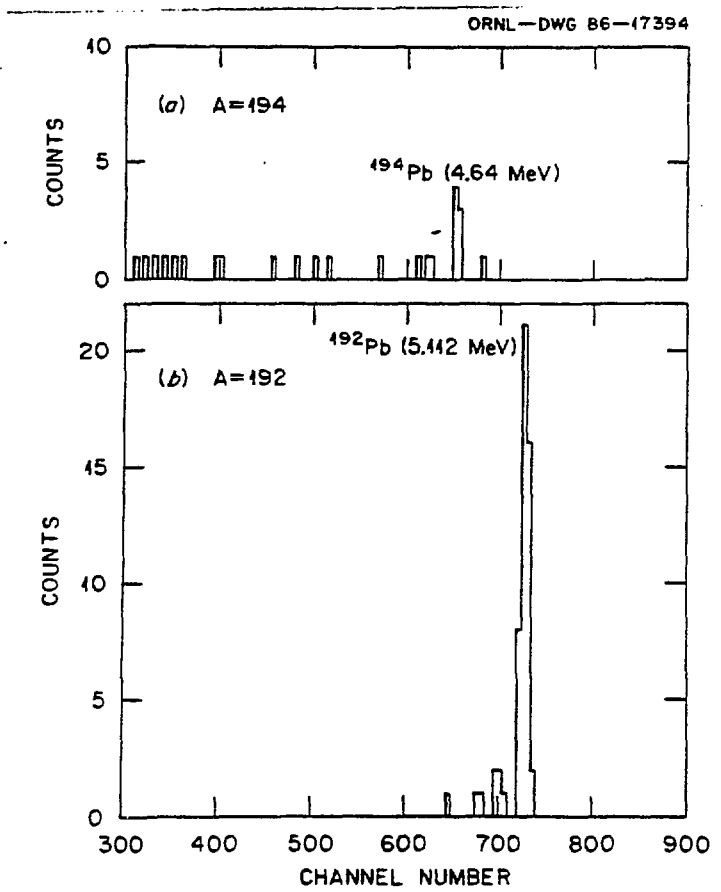


Fig. 4. Alpha-particle spectra measured for A = 194 [part (a)] and A = 192 [part (b)] radioactivities.

(A related explanation may be the varying shapes of Pb, Hg, and Pt isotopes in this mass region, i.e.,  $\alpha$  decay between the slightly oblate Pb and Hg ground states is not as hindered as it is between the oblate Hg and the prolate Pt ground states.) If correct, this suggestion implies that widths for lead nuclides with  $A > 192$  should first come closer to, and then, for larger neutron numbers, fall below mercury values.

A major difficulty in confirming this expectation arises because  $\alpha$ -decay energies decrease with increasing  $N$  and the concomitant  $\alpha$  branching ratios become extremely small. In fact, the  $\alpha$  decay of  $^{194}\text{Pb}$  had not been observed. We decided to search for  $^{194}\text{Pb}$   $\alpha$  emission and to determine the nuclide's  $\alpha$ -branching ratio by examining its (E.C. +  $\beta^+$ ) decay scheme in detail. Available data<sup>8</sup> list only a 204-keV transition in  $^{194}\text{Pb}$  decay.

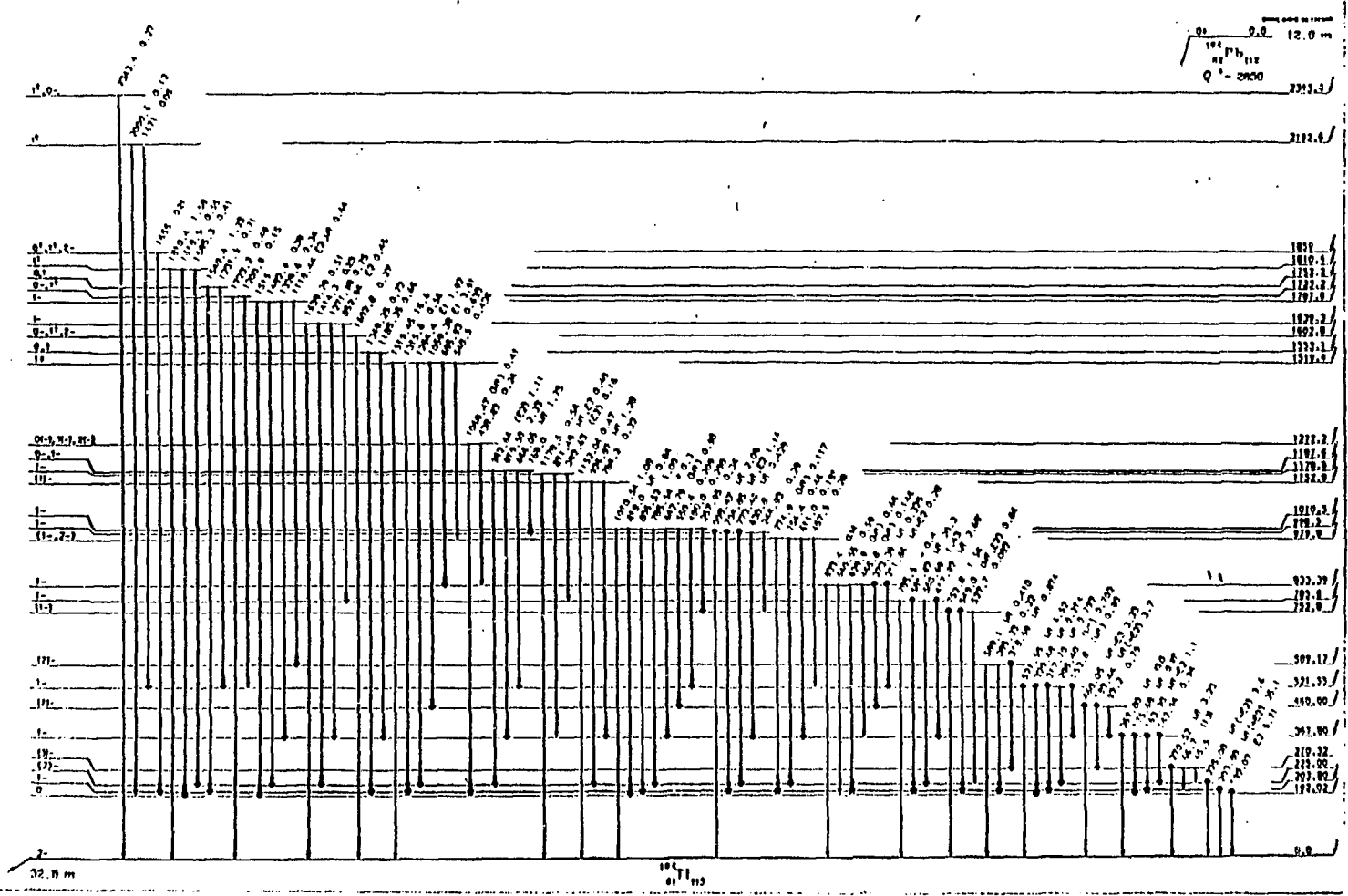


Fig. 5. Decay scheme of  $^{194}\text{Pb}$ . Gamma-ray energies are accompanied by total transition intensities and by multiplicities where available. Coincidences are indicated by dots placed at the top and bottom of transition lines.



To this end we produced  $^{194}\text{Pb}$  in bombardments of natural W with  $^{160}\text{O}$  ions from the HHIRF tandem accelerator. Following mass separation at the University Isotope Separator On-line at Oak Ridge (UNISOR) facility, the isotope's decay properties were investigated with the use of  $\gamma$ -ray, x-ray, electron, and  $\alpha$ -particle detectors. The  $\alpha$  decay energy of  $^{194}\text{Pb}$  was measured to be  $4.64 \pm 0.02$  MeV. This is illustrated in Fig. 4(a) where the  $\alpha$ -particle spectrum measured for  $A = 194$  is shown. Sources of  $^{240}\text{Pu}$  and  $^{244}\text{Cm}$  were used as calibration standards. As a check of the geometry used and to provide an additional energy calibration point, the  $^{192}\text{Pb}$   $\alpha$ -decay branching ratio<sup>9</sup> was also measured with the same experimental setup. The  $A = 192$  spectrum is displayed in Fig. 4(b). A comprehensive  $\beta$ -decay scheme (Fig. 5) was constructed by using  $\gamma$ - $\gamma$  and e- $\gamma$  coincidence data and transition energies and intensities. As indicated in Fig. 5, it incorporates 91  $\gamma$ -ray transitions into a scheme of 29 excited levels built on the  $2^-$   $^{194}\text{Tl}$  ground state. Based on this information and on the absolute  $\alpha$ -particle and  $\gamma$ -ray intensities, the  $^{194}\text{Pb}$   $\alpha$ -branching ratio was determined to be  $(7.3 \pm 2.9) \times 10^{-8}$ .

The  $^{194}\text{Pb}$  width (see Fig. 1) calculated with these data is much less than those of nuclei with  $N < 110$  and is less than that of  $^{190}\text{Pt}$  ( $N = 112$ ). The indication is that the  $Z = 82$  gap is being restored for  $N > 112$ . The  $\alpha$  widths for  $^{190}\text{Hg}$  and  $^{192}\text{Hg}$  need to be determined to be certain about this proposal; if correct, then the  $^{192}\text{Hg}$  width should be larger than that of  $^{194}\text{Pb}$ . We also show in Fig. 1 an estimated width (0.060 MeV) for  $^{184}\text{Pb}$  based on the data of Schrewe et al.<sup>10</sup> and on the assumption of an  $\alpha$  branch of 100%. [From gross  $\beta$ -decay theory<sup>11</sup> the calculated partial half-life for  $^{184}\text{Pb}$  ( $\beta^+ + \text{EC}$ ) decay is (5 - 10) seconds which yields an  $\alpha$  branching of (89 - 96%) and a  $\delta^2$  value of (0.053 - 0.057 MeV.)] This  $\delta^2$  value is appreciably smaller than the  $^{186,188,190}\text{Pb}$  widths and may indicate that the influence of the  $Z = 82$  shell is also beginning to retard the  $\alpha$  decay of extremely neutron-deficient Pb isotopes, i.e., those with  $N < 102$ .

#### IV. Reduced Widths for Nuclei with $84 < N < 100$

The  $\alpha$ -decay properties of medium-weight isotopes for elements below lead have now been investigated for about 40 years, and the known number of these  $\alpha$  emitters has increased steadily as more and more heavy-ion accelerators have gone into operation. Together with the expansion in numbers there has been an increase of reliable branching ratios so that the analysis of  $\alpha$ -decay rates for these neutron-deficient nuclides has become more instructive.

In Fig. 6 we show s-wave widths for nuclei with  $60 < Z < 80$ . The Pt and Hg data are included to provide a visual continuity with Fig. 1. The data here are not as copious as they are for the heavier elements. Nevertheless, one sees the same effect due to  $N = 82$  as the one noted earlier at  $N = 126$ , i.e., the  $\delta^2$  values peak at about four neutrons above the shell closure. The widths then decrease as the neutron numbers begin to increase in the direction

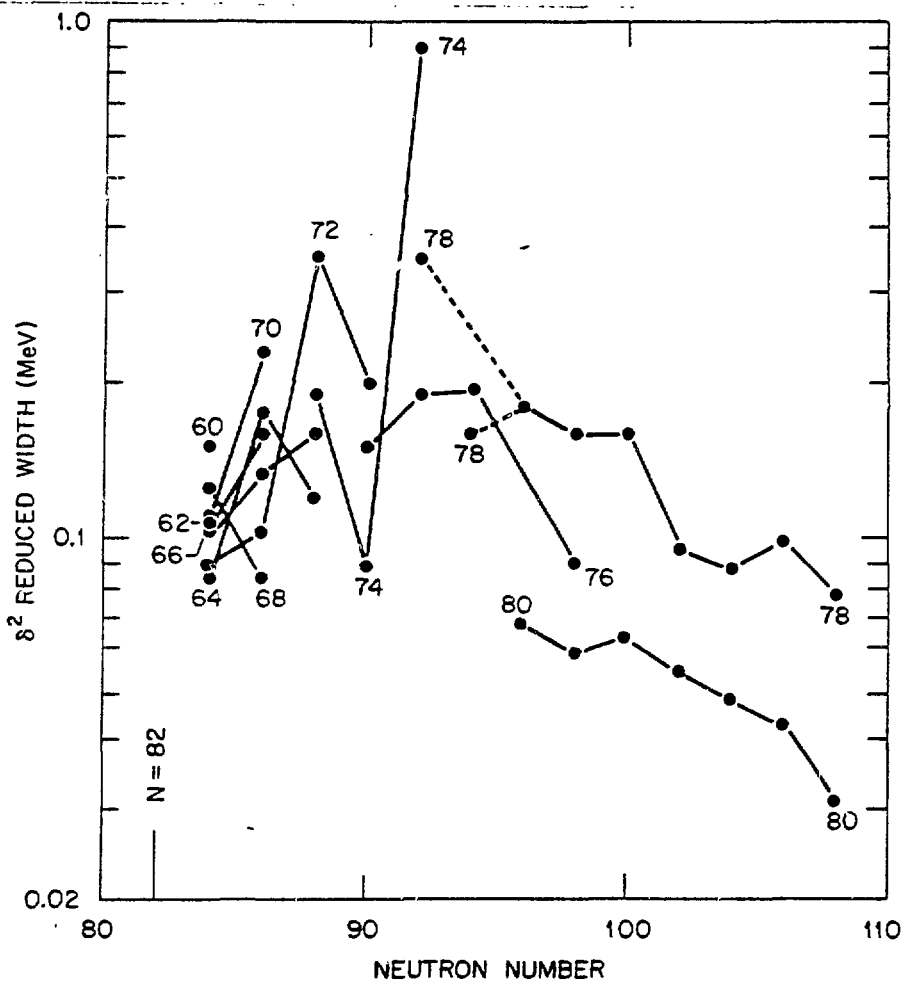


Fig. 6. Reduced widths for s-wave  $\alpha$  transitions of even-even nuclei with  $60 < Z < 80$ .

of  $N = 126$ . Only in the case of Er nuclei is the  $N = 86$  ( $^{154}\text{Er}$ ) value lower than that of the  $N = 84$  ( $^{152}\text{Er}$ ) nuclide. As noted in the original work<sup>12</sup> the  $\alpha$  branch measured for  $^{154}\text{Er}$  is undoubtedly low due to the presence  $^{155}\text{Er}$  in the sources used in determining the  $\alpha$ /total branching ratios.

No rare earth  $\alpha$  emitters with  $N < 84$  have been identified since the 82-neutron shell causes a large drop in the  $Q_\alpha$  values for these nuclei. Also, the proximity of the proton drip line raises both  $Q_{EC}$  values and probabilities for delayed and direct proton emission. Only when one gets down to the proton-rich Te and Xe nuclides does  $\alpha$  decay become once again observable. However, just one experimental  $\alpha$  branch<sup>13</sup> for an s-wave transition is available in that mass region, namely that of  $^{108}\text{Te}$ . The corresponding width,  $\sim 0.4$  MeV, is consistent with values for the  $N > 82$  nuclei shown in Fig. 6.

The existence of the  $Z = 64$  subshell was established some three decades ago on the basis of  $Q_\alpha$  systematics for  $N = 84$  nuclei. More recently the closure was also noted<sup>14</sup> in the  $\alpha$ -decay rates for the